Structural phase transition in the ordered fluorides $M^{II}ZrF_6$ (M^{II}=Co,Zn). III. Landau theory

1990 J. Phys.: Condens. Matter 2 7395

(http://iopscience.iop.org/0953-8984/2/36/003)

J. Phys.: Condens. Matter 2 (1990) 7395–7406. Printed in the UK

Structural phase transition in the ordered fluorides $M^{II}ZrF_6$ (M^{II} = Co, Zn): III. Landau theory

V Rodriguez and M Couzi
Laboratoire de Spectroscopie Moléculaire et Cristalline (URA 124 CNRS), Université de Bordeaux I, 33405 Talence Cédex, France

Received 6 February 1990, in final form 8 May 1990

Abstract. The $Fm\bar{3}m \leftrightarrow R\bar{3}$ phase transition of $M^{II}ZrF_6$ fluorides (M^{II} = Co, Zr) is analysed by means of a microscopic model, developed in the framework of Landau theory, including two coupled order parameters, namely the elastic strain with F_{2g} symmetry, and the $M^{II}(Zr)F_6$ octahedra rotation coordinate. The model is able to account for the first-order type of this transition, together with its 'improper' ferroelastic character. In addition, expressions are derived to account for the static and dynamic properties of the order parameters, which are able to reproduce consistently the experimental data obtained in the previous two papers.

1. Introduction

The first-order structural phase transition occurring in ordered fluorides with formula $M^{II}ZrF_6$ (M^{II} = Co, Zn) has been studied by means of neutron and x-ray diffraction [1] as well as Brillouin and Raman scattering measurements [2]. From the experimental results so obtained, it has been shown that the transition connects a high-temperature cubic phase, of the ordered ReO_3 type [3], with space group $Fm\bar{3}m$, to a low-temperature rhombohedral modification, with space group $R\bar{3}$. Furthermore, it has been concluded that the transition is ferrodistortive and 'improper' ferroelastic, driven by $M^{II}(Zr)F_6$ octahedra rotations. The lattice instability is induced by zone-centre rotatory soft modes, so that the transition mechanism is essentially of displacive nature. However, an order–disorder contribution may also take place in the close vicinity of the transition temperature [1, 2].

The purpose of this paper (III), which is the last one of the series, is to describe the $Fm\bar{3}m \leftrightarrow R\bar{3}$ phase transition of $M^{II}ZrF_6$ ordered fluorides by means of a microscopic model developed in the framework of Landau theory. This model includes two coupled order parameters, e and R, corresponding respectively to the F_{2g} strain and the F_{1g} rotatory coordinate of the octahedra, the temperature dependence of which has been measured by means of neutron diffraction experiments [1]. Then, a phase diagram is obtained, including the cubic phase $Fm\bar{3}m$ ($e = 0$, $R = 0$) and two different rhombohedral phases, with $R\bar{3}m$ ($e \neq 0$, $R = 0$) and $R\bar{3}$ ($e \neq 0$, $R \neq 0$) symmetries, which makes possible the occurrence of a first-order transition from $Fm\bar{3}m$ to $R\bar{3}$, as observed experimentally. The susceptibilities of the order parameters will also be considered through this model, and compared to the Brillouin and Raman scattering results [2]; hence, the mutual consistency of all experimental data will be established.

0953-8984/90/367395 + 12 $03.50

2. The model

2.1. Basic statements

From general group-theoretical considerations [2], the $Fm\bar{3}m \leftrightarrow R\bar{3}$ phase transition involves at least two order parameters, let us say η and ξ, with F_{1g} and F_{2g} symmetry respectively. This comes merely from the fact that compatibility relations between $Fm\bar{3}m$ and $R\bar{3}$ space groups lead to the following correlation schemes, $F_{1g} \rightarrow A_g + E_g$ and $F_{2g} \rightarrow A_g + E_g$, so that each one of F_{1g} and F_{2g} representations of $Fm\bar{3}m$ contains the unity representation (A_g) of $R\bar{3}$. A non-linear coupling term, i.e. an invariant of the form $\eta^2\xi$, may exist because the symmetrised square of the F_{1g} representation (η^2) contains $F_{2g}(\xi)$ ($[F_{1g}]^2 = A_{1g} + E_g + F_{2g}$; similarly, it is found that $[F_{2g}]^2 = A_{1g} + E_g + F_{2g}$). On the other hand, the F_{1g} representation fulfils the Landau criterion, since the symmetrised cube does not contain the unity representation of the space group ($[F_{1g}]^3 = A_{2g} + 2F_{1g} + F_{2g}$). In contrast, the order parameter ξ with F_{2g} symmetry determines the presence of a cubic polynomial in the free-energy expansion ($[F_{2g}]^3 = A_{1g} + F_{1g} + F_{2g}$). Finally, both order parameters η and ξ satisfy the Lifschitz condition according to which the antisymmetrised square of the corresponding representation must not contain the representation of a vector ($\{F_{1g}\}^2 \equiv \{F_{2g}\}^2 = F_{1g}$).

Let us now consider the specific characteristics of the $Fm\bar{3}m \leftrightarrow R\bar{3}$ phase transition in $M^{II}ZrF_6$ compounds. Three order parameters, which completely describe the extent of lattice distortion through the phase transition, have been determined [1, 2]:

(i) The spontaneous strain e_s, related to the strain tensor components with F_{2g} symmetry in the parent phase $Fm\bar{3}m$.

(ii) The internal deformation of the $M^{II}(Zr)F_6$ octahedra, specified by a coordinate Q with F_{2g} symmetry.

(iii) The rotation of the $M^{II}(Zr)F_6$ octahedra around the threefold axis, specified by a coordinate R with F_{1g} symmetry.

Thus, a complete expansion of the Landau free energy will include these three order parameters, which can couple to each other either linearly (eQ) or non-linearly (eR^2 and QR^2). In fact, we shall not consider such a complex thermodynamic potential since the ν_5 bending mode of the octahedra, associated with the order parameter Q, behaves as a 'hard' mode [2]. This is related to the very small values of Q measured in the rhombohedral phase, and means that the corresponding potential is quasi-harmonic. This quasi-harmonic potential, developed in terms of a harmonic part of the form $\frac{1}{2}M_E\omega_E Q^2$ slightly perturbed by anharmonic coupling terms between Q and e (see section 2.5) will be considered separately, in order to account for the splitting of the ν_5 mode in the rhombohedral phase. Thus, we are left with a free-energy expansion including two coupled order parameters e (F_{2g}) and R (F_{1g}).

2.2. The free-energy expansion

The preceding statements completely determine the form of the free-energy expansion and according to standard group-theoretical procedure, we write

$$\begin{aligned}\Delta\Phi(e_iR_j) = {} & \tfrac{1}{2}A_1(e_4^2 + e_5^2 + e_6^2) - \tfrac{1}{3}Be_4e_5e_6 + \tfrac{1}{4}C(e_4^4 + e_5^4 + e_6^4) \\ & + \tfrac{1}{2}D(e_4^2e_5^2 + e_4^2e_6^2 + e_5^2e_6^2) + \tfrac{1}{2}A_2(R_1^2 + R_2^2 + R_3^2) \\ & + \tfrac{1}{4}F(R_1^4 + R_2^4 + R_3^4) + \tfrac{1}{2}G(R_1^2R_2^2 + R_1^2R_3^2 + R_2^2R_3^2) \\ & + H(e_4R_2R_3 + e_5R_1R_3 + e_6R_1R_2) + \dots . \end{aligned} \tag{1}$$

In this expression, e_4, e_5 and e_6 are the three components of the F_{2g} strain tensor, and R_1, R_2 and R_3 are the three components of $R(F_{1g})$. For the sake of simplification, biquadratic coupling terms of the form e^2R^2 have been omitted; also, the A_{1g} ($e_1 + e_2 + e_3$) and E_g ($2e_1 - e_2 - e_3$, $e_2 - e_3$) strain tensor components as well as their coupling terms with R are not considered, since these quantities are not directly related to the transition mechanism [1, 2].

We shall restrict ourselves to the discussion of rhombohedral solutions of the form [4, 5]

$$\begin{aligned} e_4 &= \pm e_5 = \pm e_6 = \pm (1/\sqrt{3})e \\ R_1 &= \pm R_2 = \pm R_3 = \pm (1/\sqrt{3})R \end{aligned} \tag{2}$$

which means that we consider an effective potential $\Delta\Phi(e, R)$ such as

$$\Delta\Phi(e, R) = \tfrac{1}{2}A_1e^2 - \tfrac{1}{3}B'e^3 + \tfrac{1}{4}C'e^4 + \tfrac{1}{2}A_2R^2 + \tfrac{1}{4}F'R^4 + H'eR^2 \tag{3}$$

where

$$\begin{aligned} B' &= \pm (1/3\sqrt{3})B \qquad & C' &= \tfrac{1}{3}(C + 2D) \\ F' &= \tfrac{1}{3}(F + 2G) \qquad & H' &= \pm (1/\sqrt{3})H. \end{aligned}$$

The sign of B' depends only on the domain considered. The sign of H' depends on the relative directions of the strain and of the octahedra rotation. So, the combinations $B' > 0$, $H' > 0$ and $B' < 0$, $H' < 0$ on the one hand and $B' > 0$, $H' < 0$ and $B' < 0$, $H' > 0$ on the other correspond respectively to energetically equivalent solutions. In the following, we shall consider only the non-equivalent combinations $B' > 0$, $H' > 0$ and $B' > 0$, $H' < 0$; this choice of $B' > 0$ means that, in the rhombohedral phase, the minimum of the potential will correspond to a positive value of the spontaneous strain e_s as defined in paper I [1]. Finally, in order to achieve the stability of the potential with respect to the elastic strain and to the rotatory mode, we put $C' > 0$ and $F' > 0$.

2.3. The phase diagram

The crystalline phase that is stable at a given temperature corresponds to the absolute minimum of $\Delta\Phi$ (e, R); in particular, this implies the cancellation of the first derivatives:

$$\begin{aligned} \partial\Delta\Phi/\partial e &= (A_1 - B'e + C'e^2)e + H'R^2 = 0 \\ \partial\Delta\Phi/\partial R &= (A_2 + F'R^2)R + 2H'eR = 0. \end{aligned} \tag{4}$$

This system of coupled equations determines the existence of three distinct phases: phase I ($e = R = 0$) corresponds to the cubic parent phase $Fm\bar{3}m$, phase II ($e \neq 0$, $R = 0$) to a rhombohedral modification with $R\bar{3}m$ space group and phase III ($e \neq 0$, $R \neq 0$) to the rhombohedral phase $R\bar{3}$ observed experimentally.

Figure 1 shows the phase diagram (represented in the A_1, A_2 plane) as determined from model (3) with $B' > 0$ ($e_s > 0$) and $H' < 0$ (see section 2.4 for the justification of the sign of H'). This phase diagram can be compared with those previously determined from similar potentials [6–9].

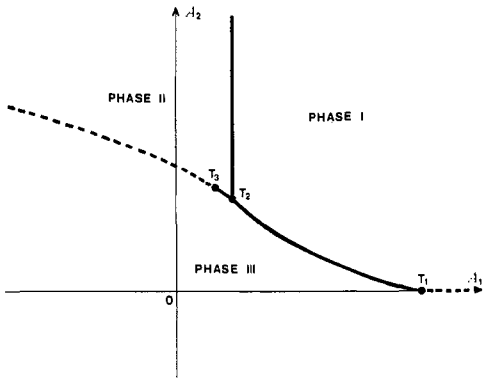

Figure 1. The phase diagram obtained with the model potential (3), with $B' > 0$ and $H' < 0$. Full curves and broken curves represent first-order and second-order phase transitions, respectively.

Since the $Fm\bar{3}m \leftrightarrow R\bar{3}$ transition is driven by octahedra rotations [2], we put

$$A_2 = a_2(T - T_0) \tag{5}$$

where a_2 is a positive constant and T_0 is the critical temperature. On the other hand, due to the 'improper' ferroelastic character of this transition [2], we put

$$A_1 = C_{44}^0 = \text{constant} \tag{6}$$

where C_{44}^0 is the 'bare' elastic constant associated with the F_{2g} strain. As usual, all other coefficients of the free-energy expansion are supposed to be temperature-independent. Now, from figure 1, it appears that a first-order transition I $\leftrightarrow$ III as observed experimentally is possible, provided that $A_1 = C_{44}^0$ lies between the values corresponding to the points T_1 and T_2, i.e.

$$\frac{2B'^2}{9C'} < A_1 < \frac{2B'^2}{9C'} + \frac{2H'^2}{F'}.$$

According to this choice for the coefficients, together with the fact that phase I is stable in a wide temperature range, phase II is not expected to occur at all; thus, the static and dynamic properties of the order parameters in phase II will not be developed in the following.

2.4. *Static properties of the order parameters*

In the parent phase I ($Fm\bar{3}m$), the spontaneous values of the order parameters e and R are always zero:

$$e_s = R = 0. \tag{7}$$

In phase III ($e_s \neq 0$, $R \neq 0$) with $R\bar{3}$ space group, the equilibrium values of e and R are determined from the set of equations (3) and (4). From (4), it follows that

$$e_s = (A_2 + F'R^2)/-2H' \qquad \text{or} \qquad R^2 = (-2H'e_s - A_2)/F'. \tag{8}$$

With the choice of $B' > 0$ we have adopted (equivalent to $e_s > 0$), it is clear that the stability conditions of phase III require, in particular, $H' < 0$.

Now, from equations (8), it is possible to write the potential (3) as a function of a unique variable, e or R, which leads to an expansion up to the eighth order in R or, more conveniently, up to the fourth order in e:

$$\Delta\Phi[T,e,R(e)] = \tfrac{1}{4}C'e^4 - \tfrac{1}{3}B'e^3 + \tfrac{1}{2}(A_1 - 2H'^2/F')e^2 - (H'/F')A_2 e - A_2^2/4F'. \tag{9}$$

The solution ($e_s > 0$) of the cubic equation that minimises the potential (9) does not have a simple algebraic form and an approximate relation will be considered in section 3.1, in order to account more easily for the variation of e_s with temperature in phase III.

2.5. *Susceptibilities of the order parameters*

In the cubic phase I, the frequency of the triply degenerate rotatory soft mode with F_{1g} symmetry is given by [10, 11]

$$\omega^2_{F_{1g}} = \omega_1^2 = \omega_2^2 = \omega_3^2 = (a_2/M_E)(T - T_0) \tag{10}$$

where M_E is the effective mass of the oscillator.

Similarly, in the rhombohedral phase III ($R\bar{3}$), for the A_g mode one can write

$$\omega^2_{A_g} = \omega_1^2 = (2F'/M_E)R^2 \tag{11a}$$

or

$$\omega^2_{A_g} = \omega_1^2 = -(2/M_E)(A_2 + 2H'e_s) \tag{11b}$$

and for the E_g mode

$$\omega^2_{E_g} = \omega_2^2 = \omega_3^2 = (1/M_E)[\tfrac{3}{2}A_2 + (\tfrac{1}{2} + F/F')R^2] \tag{12a}$$

or

$$\omega^2_{E_g} = \omega_2^2 = \omega_3^2 = (1/M_E)[(1 - F/F')A_2 - H'(1 + 2F/F')e_s]. \tag{12b}$$

Now, the adiabatic elastic constant [11, 12] C_{44} in the parent phase I is given by

$$C_{44} = C_{55} = C_{66} = A_1 = C_{44}^0 \tag{13}$$

which is in agreement with the experimental data [2]. Similarly, in the rhombohedral phase III it is

$$C_{44} = C_{55} = C_{66} = C_{44}^0 + (C + \tfrac{2}{3}D)e_s^2 - 2H'^2R^2/(A_2 + (F + \tfrac{2}{3}G)R^2) - H'^2R^2/(\tfrac{2}{3}GR^2 + H'e_s). \tag{14}$$

Here, the elastic constants are defined according to the pseudo-cubic unit cell [1]. Unfortunately, no experimental data are available for C_{44} in the rhombohedral phase.

2.6. *The quasi-harmonic potential for the ν_5 bending mode of the octahedra*

As stated above (see section 2.1) the quasi-harmonic potential V_a for the ν_5 'hard' mode of the octahedra (symmetry F_{2g}), relative to the coordinate Q [1], is developed in terms

of a harmonic potential V_h, slightly perturbed by anharmonic coupling terms V_c between the coordinate Q and the elastic strain components with the same symmetry:

$$V_a(Q_i, e_j) = V_h(Q_i) + V_c(Q_i, e_j). \tag{15}$$

According to standard group-theoretical procedure, it follows that

$$V_h(Q_i) = \tfrac{1}{2}M'_E\omega'^2_E(Q_1^2 + Q_2^2 + Q_3^2) \tag{16}$$

$$\begin{aligned} V_c(Q_i, e_j) = {} & I(Q_1e_4 + Q_2e_5 + Q_3e_6) + J(Q_1e_5e_6 + Q_2e_4e_6 + Q_3e_4e_5) \\ & + K(Q_1Q_2e_6 + Q_1Q_3e_5 + Q_2Q_3e_4) + \tfrac{1}{2}L(Q_1^2e_4^2 + Q_2^2e_5^2 + Q_3^2e_6^2) \\ & + N(Q_1Q_2e_4e_5 + Q_1Q_3e_4e_6 + Q_2Q_3e_5e_6) + \ldots \end{aligned} \tag{17}$$

where M'_E and ω'_E are the effective mass and the frequency of the oscillator, respectively, Q_1, Q_2 and Q_3 the three components of the triply degenerate coordinate Q, and e_4, e_5 and e_6 the elastic strain components with F_{2g} symmetry (see equation (1)).

In the rhombohedral phase, $R\bar{3}$, we have

$$Q_1 = \pm Q_2 = \pm Q_3 = \pm (1/\sqrt{3})Q \tag{18}$$

and this potential, developed up to the fourth order (terms of the form Q^2e^2) is stable in this phase as long as $L + 2N > 0$.

The equilibrium value of the coordinates Q can be obtained by introducing V_a (15) in the thermodynamic potential (1). If we assume that the bilinear coupling terms of the form Qe are predominant in (17) (higher-order coupling terms are neglected here), then we obtain a direct proportionality relation between Q and e_s in the rhombohedral phase:

$$Q = (I/M'_E\omega'^2_E)e_s. \tag{19}$$

Of course, in the cubic phase I, we have $Q = e_s = 0$. Note that this procedure leads to a small renormalisation of the A_1 coefficient in (3), which has been neglected in the preceding sections.

Taking account of equations (2), the frequency of the F_{2g} ν_5 mode in the cubic phase $Fm\bar{3}m$ is

$$\omega'^2_{F_{2g}} = \omega'^2_1 = \omega'^2_2 = \omega'^2_3 = \omega'^2_E. \tag{20}$$

In the rhombohedral phase $R\bar{3}$, one obtains for the A_g mode

$$\omega'^2_{A_g} = \omega'^2_1 = \omega'^2_E + (1/M'_E)[2K'e_s + (L + 2N)e_s^2] \tag{21}$$

and for the E_g mode

$$\omega'^2_{E_g} = \omega'^2_2 = \omega'^2_3 = \omega'^2_E + (1/M'_E)[-K'e_s + (L - N)e_s^2] \tag{22}$$

where $K' = K/\sqrt{3}$.

3. Comparison with experimental data

The equations established in section 2 from the model potentials (1) and (15) must be able to reproduce the static properties and susceptibilities of the order parameter e, R and Q, through the $Fm\bar{3}m \leftrightarrow R\bar{3}$ phase transition. The discussion will now be focused on the case of $CoZrF_6$, where most of these quantities could be measured in both the

cubic and rhombohedral phases [1, 2]. All fits have been performed with the help of computer programs using a least-squares and/or Newton–Raphson iterative method.

3.1. Approximate equation for the temperature dependence of the spontaneous strain e_s

As mentioned previously, a convenient algebraic form for the temperature dependence of the spontaneous strain e_s in the rhombohedral phase $R\bar{3}$ cannot be derived from equation (9) because of the e^3 cubic term in the free-energy expansion. Approximate relations have been considered already in the case of a similar potential developed for the 'trigger'-type [13] phase transition of benzyl [14].

In the case of $M^{II}ZrF_6$ compounds, a first-order $Fm\bar{3}m \leftrightarrow R\bar{3}$ transition can be accounted for by a simplified potential of the form [9]:

$$\Delta\Phi(T, R, e) = \tfrac{1}{2}\alpha(T - T_0)R^2 - \tfrac{1}{4}\beta R^4 + \tfrac{1}{6}\gamma R^6 + \tfrac{1}{2}C_{44}^0 e^2 - \lambda e R^2 \qquad (23)$$

where all coefficients are positive and constant.

It should be pointed out that this potential is incomplete. Indeed, the introduction of the R^6 term is equivalent to a development up to the third order in e, because of the coupling term eR^2, but at the same time, we neglect in (23) the e^3 invariant allowed by symmetry. Nevertheless, let us minimise (23) with respect to e and R; then one obtains for the rhombohedral phase

$$e_s = \frac{\beta' + [\beta'^2 - 4\alpha\gamma(T - T_0)]^{1/2}}{2\gamma} \frac{\lambda}{C_{44}^0} \qquad (24)$$

and

$$R^2 = (C_{44}^0/\lambda)e_s \qquad (25)$$

with

$$\beta' = \beta + (2\lambda^2/C_{44}^0) \qquad (\beta' > 0).$$

In a first step, we have fitted the experimental values of the spontaneous strain e_s in $CoZrF_6$ (this is the quantity where the best accuracy is obtained) with the help of equation (24). The result obtained with the following set of coefficients:

$$e_s = 6.16 \times 10^{-3} + (6.843 \times 10^{-4} - 2.40 \times 10^{-6}T)^{1/2} \qquad (26)$$

is shown in figure 2; the agreement between calculated and observed values is quite satisfactory. However, the coefficients so obtained cannot be related to those appearing in the model potential (3). Clearly, relation (26) must be considered as a semi-empirical equation, able to reproduce the thermal evolution of e_s in the rhombohedral phase.

Now, from equation (26), we have tried to adjust the values of R using relation (25). This gives

$$R^2(m^2) = 5.82 \times 10^{-20} e_s. \qquad (27)$$

As shown in figure 3 (broken curve), the agreement with experimental data is rather poor; this is a clear illustration of the incompleteness of the potential (23). There is not a direct proportionality relation between R^2 and e_s as given by equation (25), which probably has to be related to the fact that the $Co(Zr)F_6$ octahedra are not perfect rigid bodies [1].

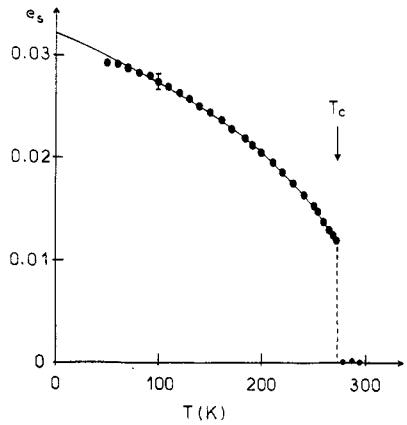

Figure 2. The thermal evolution of the spontaneous strain in $CoZrF_6$. Circles are experimental points taken from [1] and the full curve represents the best fit according to equation (26).

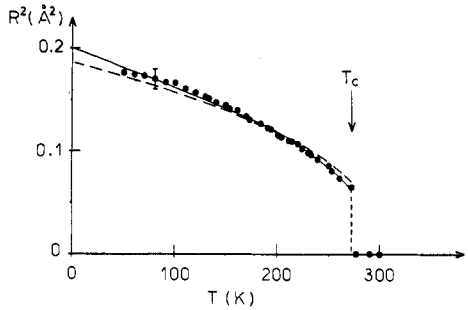

Figure 3. The thermal evolution of the coordinate R in $CoZrF_6$. Circles are experimental points taken from [1]; the broken curve and full curve represent the best fits according to equation (27) and equation (28), respectively.

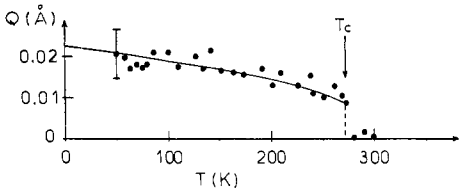

Figure 4. The thermal evolution of the coordinate Q in $CoZrF_6$. Circles are experimental points taken from [1] and the full curve represents the best fit according to equation (29).

3.2. *The static properties of the order parameters R and Q*

With the help of the semi-empirical equation (26), it is now possible to fit all other interesting quantities, according to the model potential (1). So, the fit of R values after relations (5), (8) and (26) leads to the result

$$R^2(m^2) = 5.68 \times 10^{-20}\, e_s - 0.76 \times 10^{-24}(T - 205). \tag{28}$$

The agreement between calculated and measured values is now much more satisfactory (figure 3, full curve). From this fit, a number of coefficients have been evaluated, namely $T_0 = 205$ K, $a_2/F' = 0.76 \times 10^{-24}$ m^2 K^{-1} and $H'/F' = -2.84 \times 10^{-20}$ m^2; of course, all these values will be kept in following adjustments, when necessary.

Similarly, with the help of equations (19) and (26) one obtains for Q:

$$Q(\mathrm{m}) = 0.70 \times 10^{-10}\, e_s. \tag{29}$$

There are important errors in the measurements of Q values; however, the general trend for the variations of Q as a function of temperature is well reproduced by equation (29) (figure 4).

3.3. *The frequencies of the soft rotatory mode*

As mentioned previously [2], it was not possible to assign the two components of the soft rotatory mode of the octahedra in the phase $R\bar{3}$ in terms of A_g and E_g symmetry.

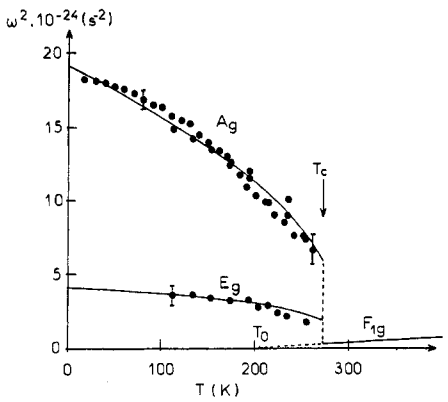

Figure 5. The thermal evolution of the soft rotatory mode frequencies in $CoZrF_6$. Circles are experimental points taken from [2] and full curves represent the best fit according to equations (30), (31) and (32) ($\omega_{A_g} > \omega_{E_g}$ in the rhombohedral phase).

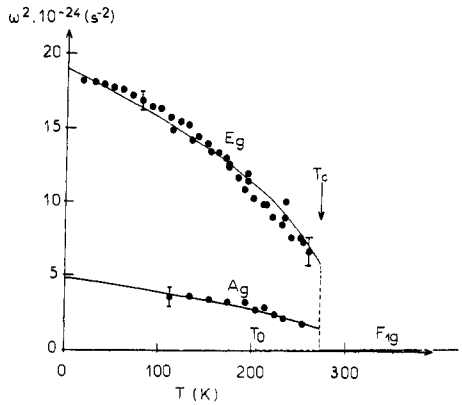

Figure 6. The thermal evolution of the soft rotatory mode frequencies in $CoZrF_6$. Circles are experimental points taken from [2] and full curves represent the best fits according to equations (33), (34) and (35) ($\omega_{E_g} > \omega_{A_g}$ in the rhombohedral phase).

Thus, the two possible assignments will be considered successively, i.e. $\omega_{A_g} > \omega_{E_g}$ and $\omega_{E_g} > \omega_{A_g}$. In both cases one has to take account of the direct proportionality relation existing between $\omega^2_{A_g}$ and R^2, as given by equation (11*a*). Then with the parameter $T_0 = 205$ K fixed (see section 3.2), the frequency ω_{E_g} is deduced from ω_{A_g} with the help of only one adjustable parameter, namely F/F' (see equations (12*a*) and (12*b*)).

(i) $\omega_{A_g} > \omega_{E_g}$. From equations (11), (12), (26) and (28), the best fits (figure 5) are given by

$$\omega^2_{A_g}(s^{-2}) = 96 \times 10^{44} R^2 = 545 \times 10^{24} e_s - 73 \times 10^{20} (T - 205) \tag{30}$$

and

$$\omega^2_{E_g}(s^{-2}) = 149.6 \times 10^{24} e_s + 34.7 \times 10^{20} (T - 205). \tag{31}$$

All coefficients so obtained fulfil the stability conditions of the potential (3) in the rhombohedral phase. Consequently, the frequency of the inactive F_{1g} rotatory mode in the cubic phase, deduced from equation (10), is given by figure 5.

$$\omega^2_{F_{1g}}(s^{-2}) = 36.5 \times 10^{20} (T - 205). \tag{32}$$

(ii) $\omega_{E_g} > \omega_{A_g}$. Following the same procedure, the best fits to the experimental data in the rhombohedral phase (figure 6) are now given by

$$\omega^2_{A_g}(s^{-2}) = 25 \times 10^{44} R^2 = 139 \times 10^{24} e_s - 19 \times 10^{20} (T - 205) \tag{33}$$

and

$$\omega^2_{E_g}(s^{-2}) = 553.8 \times 10^{24} e_s - 59.9 \times 10^{20} (T - 205) \tag{34}$$

so that the frequency of the F_{1g} mode in the cubic phase (figure 6) is

$$\omega^2_{F_{1g}}(s^{-2}) = 9.5 \times 10^{20} (T - 205). \tag{35}$$

It should be pointed out that lattice dynamics calculations made on simple fluorides such

as AlF_3 in their rhombohedral structural modification ($R\bar{3}c$) are in accordance with case (i) [15]. However, when considering our data alone, the choice between (i) and (ii) is not obvious, since both cases lead to good fits of the experimental results (figures 5 and 6), with coefficients that fulfil the stability conditions of phase $R\bar{3}$. In fact, case (i), with $F'/F = 0.05$, corresponds to a very anisotropic potential for the rotatory mode ($F \ll G$ after equations (1) and (3)), whereas in case (ii), with $F/F' = 7.30$, this potential is much more isotropic ($F > G$).

Finally, whatever the exact assignment may be, the inferred values for the soft rotatory mode frequencies in the cubic phase are always very small ($\omega_{F_{1g}} \simeq 20\ cm^{-1}$ at 300 K in case (i) and $\omega_{F_{1g}} \simeq 10\ cm^{-1}$ at 300 K in case (ii)). This means that the corresponding potentials are rather flat, auguring for the existence of orientational disorder of the octahedra. Indeed, such a picture is in agreement with the x-ray diffuse scattering patterns observed with $CoZrF_6$ in the cubic phase [1]. Furthermore, it has been mentioned [2] that the A_g and E_g components of the rotatory mode exhibit a considerable broadening in the rhombohedral phase, just below the transition temperature, which could be due to premonitory effects of octahedra disorder [2]. Then, because of disorder, the F_{1g} mode in the cubic phase may be expected to be heavily damped or of diffusive nature; since it is optically inactive, inelastic neutron scattering experiments are necessary to confirm such a hypothesis.

3.4. The splitting of the ν_5 bending mode

According to previous data obtained with rhombohedral $CsSbF_6$ single crystal [16], the ν_5 component of highest frequency has E_g symmetry and the other one A_g. By taking the same assignment in $CoZrF_6$, the best fits to the experimental data according to equations (21), (22) and (26) gives in the rhombohedral phase

$$\omega'^2_{A_g}(s^{-2}) = 56.03 \times 10^{24} - 39.5 \times 10^{24}\, e_s + 458 \times 10^{24}\, e_s^2 \tag{36}$$

and

$$\omega'^2_{E_g}(s^{-2}) = 56.03 \times 10^{24} + 19.5 \times 10^{24}\, e_s + 3345 \times 10^{24} e_s^2 \tag{37}$$

which means that in the cubic phase (equation (20))

$$\omega'^2_{F_{2g}}(s^{-2}) = 56.03 \times 10^{24}. \tag{38}$$

The stability condition $L + 2N > 0$ is fulfilled and again the quality of the fits is quite satisfactory (figure 7).

4. Conclusions

In order to account for the $Fm\bar{3}m \leftrightarrow R\bar{3}$ phase transition occurring in $M^{II}ZrF_6$ ordered fluorides, we have developed a microscopic model that is able to reproduce consistently all experimental results obtained with $CoZrF_6$. The octahedra rotation appears clearly to be the driving order parameter for the transition. Because of the three-dimensional arrangement of the octahedra, this rotation induces a set of internal strains, resulting in a small local deformation of the octahedra and, more significantly, to a rhombohedral distortion of the unit cell. The model takes account of all these phenomena. Then, the spontaneous strain that characterises the rhombohedral phase appears to be a secondary order parameter ('improper' ferroelastic phase transition).

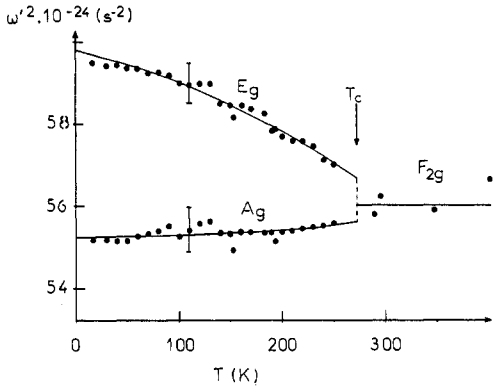

Figure 7. The thermal evolution of the frequencies of the ν_5 bending mode in $CoZrF_6$. Circles are experimental points taken from [2] and full curves represent the best fit according to equations (36), (37) and (38).

The behaviour of the soft rotatory modes in $CoZrF_6$ is well reproduced, as well as the temperature-dependent splitting of the ν_5 internal bending mode of the octahedra. Thus, the transition is essentially of displacive nature. However, an order–disorder contribution may also take place in the close vicinity of the transition temperature. Inelastic neutron scattering and neutron diffraction experiments on single crystals would be desirable to analyse such phenomena. Also, it should be pointed out that preliminary results obtained with $ZnZrF_6$ [1, 2, 9] are not at variance with the model predictions. Clearly, there exists a strong analogy in the behaviour of $CoZrF_6$ and $ZnZrF_6$ but the fits from the model are less meaningful with $ZnZrF_6$ [9] because a number of important experimental data are still missing.

Finally, the model with two coupled order parameters predicts the existence of another rhombohedral phase with space group $R\bar{3}m$, which has not been observed in $M^{II}ZrF_6$ fluorides, but seems to be stable in $BaSiF_6$ or $BaGeF_6$ [17, 18]. According to the present analysis, an eventual transition from $Fm\bar{3}m$ to $R\bar{3}m$ would be 'proper' ferroelastic; thus, $BaSiF_6$ and $BaGeF_6$ are good candidates to probe further the phase diagram deduced from the model.

Acknowledgment

The authors wish to thank Mr Philippe Maraval (Laboratoire de Spectroscopie Moléculaire et Cristalline, Université de Bordeaux I) for valuable help in handling the computer programs.

References

[1] Rodriguez V, Couzi M, Tressaud A, Grannec J, Chaminade J P and Soubeyroux J L 1990 *J. Phys.: Condens. Matter* **2** 7373–86

[2] Rodriguez V, Couzi M, Tressaud A, Grannec J, Chaminade J P and Ecolivet C 1990 *J. Phys.: Condens. Matter* **2** 7387–94

[3] Babel D and Tressaud A 1985 *Inorganic Solid Fluorides* ed P Hagenmuller (New York: Academic) p 97

[4] Stokes H T and Hatch D M 1988 *Isotropic Subgroups of the 230 Crystallographic Space Groups* (Singapore: World Scientific) pp 1-371, 13-1

[5] Toledano J C and Toledano P 1987 *The Landau Theory of Phase Transitions* (Singapore: World Scientific) p 180

[6] Gufan Yu M and Larin E S 1980 *Sov. Phys.–Solid State* **22** 270
[7] Gufan Yu M and Torgashev V I 1980 *Sov. Phys.–Solid State* **22** 951
[8] Gufan Yu M and Torgashev V I 1981 *Sov. Phys.–Solid State* **23** 656
[9] Rodriguez V 1989 *Thesis* University of Bordeaux I
[10] Cowley R A 1980 *Adv. Phys.* **29** 1
[11] Slonczewski J C and Thomas H 1970 *Phys. Rev.* B **1** 3599
[12] Rehwald W 1973 *Adv. Phys.* **22** 721
[13] Holakovsky J 1973 *Phys. Status Solidi* b **56** 615
[14] Toledano J C 1979 *Phys. Rev.* B **20** 1147
[15] Daniel P 1990 *Thesis* University of Maine, Le Mans
[16] De V Steyn M M, Heyns A M and English R B 1984 *J. Crystallogr. Spectrosc. Res.* **14** 505
[17] Hoard J L and Vincent W B 1940 *J. Am. Chem. Soc.* **62** 3126
[18] Hoskins B F, Linden A, Mulvaney P C and O'Donnel T A 1984 *Inorg. Chim. Acta* **88** 217